

Seeking for toroidal event horizons from initially stationary BH configurations

Marcelo Ponce[†]

E-mail: mponce@astro.rit.edu

Carlos Lousto[‡]

E-mail: lousto@astro.rit.edu

Yosef Zlochower[‡]

E-mail: yosef@astro.rit.edu

[†] Center for Computational Relativity and Gravitation, Rochester Institute of Technology, 85 Lomb Memorial Drive, Rochester, New York 14623, USA.

[‡] Center for Computational Relativity and Gravitation and School of Mathematical Sciences, Rochester Institute of Technology, 85 Lomb Memorial Drive, Rochester, New York 14623, USA.

Abstract. We construct and evolve non-rotating vacuum initial data with a ring singularity, based on a simple extension of the standard Brill-Lindquist multiple black-hole initial data, and search for event horizons with spatial slices that are toroidal when the ring radius is sufficiently large. While evolutions of the ring singularity are not numerically feasible for large radii, we find some evidence, based on configurations of multiple BHs arranged in a ring, that this configuration leads to singular limit where the horizon width has zero size, possibly indicating the presence of a naked singularity, when the radius of the ring is sufficiently large. This is in agreement with previous studies that have found that there is no apparent horizon surrounding the ring singularity when the ring's radius is larger than about twice its mass.

Submitted to: *Class. Quantum Grav.*

1. Introduction

The recent dramatic breakthroughs in the numerical techniques to evolve black-hole-binary (BHB) spacetimes [1–3] have led to rapid advancements in our understanding of black-hole physics. Notable among these advancements are developments in mathematical relativity, including systems of PDEs and gauge choices [4–6], the exploration of the validity of the cosmic censorship conjecture [7–12], and the application of isolated horizon (IH) formulae [8, 9, 13–16]. Recent studies include the algebraic classification of spacetime post-merger of BHBs [17, 18], investigations of the orbital mechanics of spinning BHBs [7–9, 19–22], studies of the recoil from the merger of unequal mass BHBs [23–25], the remarkable discovery of unexpectedly large recoil velocities from the merger of certain spinning BHBs [19, 26–41], investigations into the mapping between the BHB initial conditions (individual masses and spins) and the final state of the merged black hole [42–49], and improvements in our understanding of the validity of approximate BHB orbital calculations using post-Newtonian (PN) methods [50–57]. There have also been notable advances in our understanding of the small mass ratio limit, as well as hybrid perturbative/numerical methods for evolving small mass ratio BHBs [29, 58, 59].

Even before the breakthrough there were important studies of the structure of event horizons for non-stationary spacetimes. An event horizon is a 3D null hypersurface in spacetime that forms the boundary of the region of causally connected to \mathcal{I}^+ . The event horizon is actually that part of the null surface that is caustic free in the future. If two null generators cross, then prior to the crossing, the generators are not on the horizon, and a causal curve intersecting these generators can terminate on \mathcal{I}^+ . To understand why this is, we note that the region of the null hypersurface containing this crossing is equivalent to a lightcone in the local Minkowski frame. Unlike the region of the interior of the light cone in the future of the intersection point, the region in the past of the intersection point of the light cone is causally connected to the region outside the light cone. In the case of the event horizon, points on the null generators prior to a caustic are causally connected to \mathcal{I}^+ .

In Ref. [60] it was proven that, for asymptotically flat spacetimes satisfying the null energy condition, all causal (timelike or null) curves from \mathcal{I}^- to \mathcal{I}^+ are deformable to a topologically trivial curve. An important consequence of this “topological censorship” theorem is that constant time slices of an event horizon must (at least in the distant future) be topologically spherical. Hawking proved [61, 62] (see [63–65] for generalizations of this theorem to higher dimensions) that spacelike slices of event horizons in asymptotically

flat stationary spacetimes obeying the dominant energy condition have topology S^2 . For non-stationary spacetimes, toroidal horizons are allowed, but the *holes* in these horizons would close up fast enough to prevent causal curves from traversing the holes. Interestingly, the existence of a single toroidal horizon slice implies that there is a 1-parameter family of toroidal horizon slices in the neighborhood of this particular horizon slice [64].

The first numerical studies of the event horizon topologies for non-stationary spacetimes involved the axisymmetric collapse of a rotating toroidal distribution of dust [66, 67] and theoretical studies of possible horizon topologies based ellipsoidal wavefronts in Minkowski space [68]. However, as of yet, there have been no simulations published that have unequivocally shown event horizons with toroidal topologies from the mergers of multiple black holes (BHs) (see [69] for a possible example), and very few that have shown event horizons of any form (see [69, 70]). The main reason for this is that an event horizon is a global structure whose location is determined by the entire future of the spacetime (in practice, one only needs to evolve to the point where the final remnant BH equilibrates). Thus, in order to find an event horizon, one must first evolve the spacetime, obtain the full four-metric at all times in the future of the initial hypersurface, and then evolve the null generators of the last common apparent horizon (AH) backwards in time. This presents a significant storage challenge, and since much of the information about BHBs can be obtained from the AHs (using, for example, the IH formalism), such an event horizon search is seldom performed. In a typical BHB simulation, one is interested in the masses and spins of the individual BHs when they are far away and in the mass and spin of the remnant BH after it has equilibrated. In these two regimes, the IH formalism provides accurate measurements of the mass and spin of the BHs. However, near merger, where the AH and event horizon can differ significantly, the IH formalism will not produce accurate results. Moreover, the structure of the AHs will not match that of the event horizon. Thus, it is important to examine the event horizon structure in the vicinity of the merger in order to gain an understanding of how event horizons behave in highly dynamical spacetimes.

While topological censorship forbids an event horizon from remaining toroidal, it is interesting to see if purely vacuum configurations can have instantaneous toroidal slices. To partially address this question, we examine the dynamics of a spacetime with a ring-like, rather than pointlike, singularity. This configuration was first studied in [76], where it was found that an AH does not exist if the rings radius is sufficiently large, leading to the conjecture that this is a naked singularity (see also [75]). We find evidence to support this conjecture. Here we extend the analysis and show evidence that there is no common

nonsingular event horizon for sufficiently large ring radii.

While our proposed configuration would not violate cosmic censorship because the singularity does not develop in the future of a non-singular slice (i.e. all slices contain a singularity), questions concerning the validity of the cosmic censorship are also quite interesting. The authors of Ref. [71, 72] evolved a prolate spheroidal distribution of collisionless gas and found that generically, for large enough spheroids, a singular spindle forms on the long axis of the spheroid which is apparently naked, violating cosmic censorship. In a follow-up work in Ref. [73] they found vacuum configurations of linear black-hole distribution like the ones we use here also contain naked singularities for sufficiently long lines. In [74], the authors found that naked singularities can form in 5-dimensional black-string configurations.

In this paper we use the following nomenclature. While the event horizon is a global 3-d hypersurface in a 4-d space, we are interested in spacelike slices of the horizon. That is if Σ_t is a one-parameter family of spacelike slices that foliates the space time and \mathcal{H} is the event horizon, then we are interested in the object $\mathcal{H}_t = \Sigma_t \cap \mathcal{H}$ (which may be a disconnected set). In the sections below we refer to these spatial slices of the event horizon (\mathcal{H}_t) as “EHs”. We note that for well separated BHs these “EHs” will also be AHs. In order to locate these distinct EHs we track the null generators using the EHFinder Cactus thorn [69], backwards in time, dropping those generators that have crossed, leaving only those generators still on the EH.

This paper is organized as follows. In Sec. 2 we discuss the ring configuration and toroidal event horizons. In Sec. 2.1 we discuss the initial data for the numerical simulations. In Sec. 3 we discuss the numerical techniques. In Sec. 4 we discuss the EHs found for the discrete ring and discrete line cases, as well as the AHs found for the continuum ring. Finally, in Sec. 5 we discuss the implication of our numerical results and speculate about the nature of the EH for the continuum ring.

2. Toroidal Event Horizons and Black Hole Rings

While topological censorship requires that the 3-d hypersurface corresponding to the event horizon is simply connected, there is no such restriction on 2-dimensional spatial slices of the event horizon. The question we wish to address in this paper is, can a configuration of initially stationary (in the sense of having zero momentum, the spacetime itself is not stationary and does not possess a timelike Killing vector field) nonspinning black holes form a horizon with topologically toroidal slices, and if so, can we find these slices

numerically? In order to investigate these questions, we examine configurations of black holes (BHs) arranged in a ring configuration, as well configurations with BHs arranged in a line. The idea behind using a ring is that if neighboring BHs are close enough together, and the ring is wide enough, then a common event horizon (if it exists) should have a toroidal topology (on the 3-dimensional slice). We can imagine constructing such a ring by keeping the total mass fixed, while increasing the number of BHs in the ring. We might expect that, for a sufficiently large number of BHs, a common event horizon will form. However, as we conjecture below based on our numerical simulations, this event horizon may only forms in the limiting case where there is an infinite number of BHs with infinitesimal masses. The EH, while toroidal, may actually have zero width. Interestingly, we can construct initial data corresponding to this limiting distribution of BHs using the techniques of electrostatics. This configuration was studied in Ref. [76], as well as [75], where it was shown that a common apparent horizon (AH) does not exist if the ratio of the ring radius to mass is larger than $R/M \sim \frac{20}{3\pi} \approx 2.12$.

An AH must be simply connected [64], hence the absence of an AH indicates that the EH may not be simply connected. We note that it is possible, to construct unusual slicings where the EH is spherical but an AH does not exist. However, our initial data are based on a superposition of Brill-Lindquist BHs [77], which, at least for finite numbers of BHs, does not lead to these unusual slices. In [76] it was argued that the absence on an AH indicates that this singularity is naked.

2.1. Initial Data

We construct initial data by superimposing conformally-flat, initially stationary non-spinning, black-hole (BH) configurations. That is, we take as initial data $K_{ij} = 0$ and $\gamma_{ij} = \psi^4 \delta_{ij}$, where $\Delta\psi = 0$. For the case of discrete BHs, we use an ordinary superposition of Brill-Lindquist BHs [77], while for the case of the BH ring, we use the techniques of electrostatic to solve for the potential of a 1-dimensional ring of charge.

Continuous Ring: To construct initial data for the continuous BH ring we solve

$$\Psi(\vec{r}) = M \int_0^{2\pi} \frac{d\phi'}{\sqrt{r^2 - 2rR \cos(\phi - \phi') + z^2}}, \quad (1)$$

to obtain [75, 76]

$$\Psi = 1 + \frac{M}{2\pi} \left[\frac{2K\left(\frac{-4\rho\rho_0}{z^2 + (\rho - \rho_0)^2}\right)}{\sqrt{z^2 + (\rho - \rho_0)^2}} + \frac{2K\left(\frac{4\rho\rho_0}{z^2 + (\rho + \rho_0)^2}\right)}{\sqrt{z^2 + (\rho + \rho_0)^2}} \right], \quad (2)$$

where $K(x)$ is the complete elliptical integral of the first kind, with the convention used by Mathematica

$$K(x) = \int_0^{\pi/2} \frac{d\theta}{\sqrt{1 - k \sin^2 \theta}}.$$

While initial data corresponding to arbitrary ring radii is easy to construct, actual evolutions of these data are numerically challenging for large radii, as explained below. Note that $\psi \sim \ln R$, where R is the coordinate distance to the ring, in the neighborhood of the ring singularity. Hence, the evolution variable $W = \psi^{-2}$ will have the form $W \sim 1/(\ln R)^2$, which is continuous, but not differentiable at $R = 0$.

Discrete Ring: To construct initial data for the discrete BH ring (i.e. a symmetric distribution of BHs on a ring) we superimposed N BHs, where the total mass of the ring is $1M$. Here ψ is given by

$$\begin{aligned} \psi &= 1 + \sum_{i=0}^{N-1} \frac{m_i}{|\vec{r} - \vec{r}_i|} \\ &= 1 + \sum_{i=0}^{N-1} \frac{m_i}{\sqrt{(x - x_i)^2 + (y - y_i)^2 + (z - z_i)^2}}, \end{aligned} \quad (3)$$

where $m_i = M/N$, $\vec{r}_i = [R \cos(i\alpha), R \sin(i\alpha), 0]$ is the coordinate location of BH i , R is the radius of the ring, and $\alpha = 2\pi/N$. In order to preserve reflection symmetry, N must be even.

For this configuration, the ADM mass of the spacetime is approximately $M_{\text{ADM}} = Nm$ and hence the final merged BH should have a mass of $M \sim N m$, where N is the number of BHs and m is mass of each BH. Binding energy, which tends to zero as the configuration size goes to ∞ , will reduce the ADM mass by a small amount (for example, the binding energy of a non-spinning BH binary near the ISCO is only about 2%), and gravitational radiation will further reduce the mass of the final black hole by a small percentage.

Our technique of using a discrete ring to model the horizon dynamics of a continuum ring distribution is a natural extension of the techniques developed in [73].

Line: In order to mimic the differential line element of the ring, we consider a finite line element constrained such that the average linear mass density of black holes per unit length of the line is the same as that of the ring. To construct this linear configuration of BHs, we consider a line of length L , and place N BHs on the line with a uniform separation ℓ . The outermost BHs are arranged a distance $\ell/2$ from the ends of the line. In

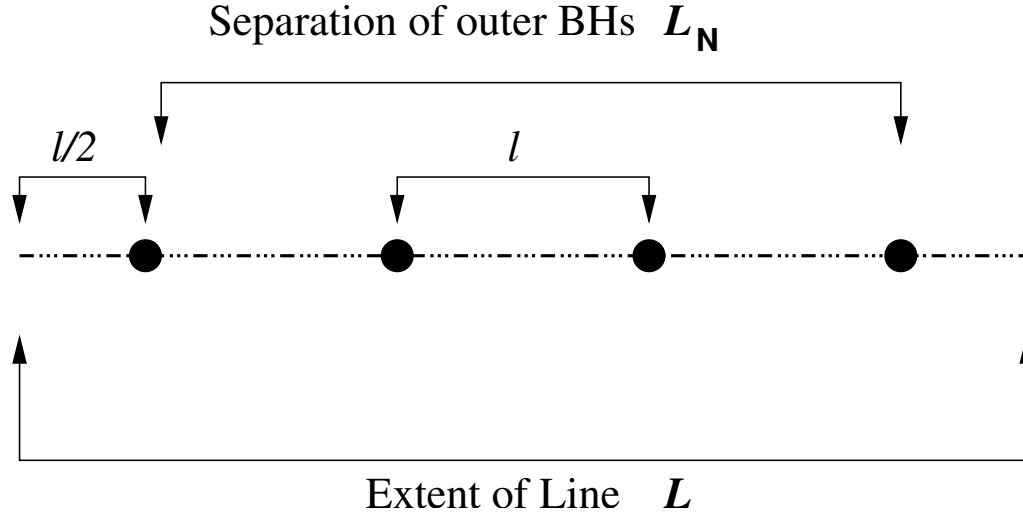


Figure 1. The setup for the linear distribution of BHs. l is the separation between neighboring BHs, L_N is the separation between the two outer BHs, while L is the length of the line. The line is formally a length l longer than the separation of the two outer BHs so that the linear density is the same in the neighborhood of each BH (we consider that the BH's mass is spread out over an interval of $\pm l/2$ around the BHs center).

this configuration, the mass density of the line is $m/\ell = M/L$, where $m = M/N$ (see Fig. 1). If L is the total length of the line and L_N is the separation between the two outer BHs, then $L = [N/(N-1)]L_N$ and the average linear density is $M/L = (N-1)m/L_N$. Hence

$$L_N = 2\pi R \frac{N-1}{N}, \quad (4)$$

where R is the radius of the ring.

Note this configuration was first studied in Ref. [73] to show that a common apparent horizon does not exist for lines larger than $L \sim 1.5M$, and to therefore argue that this configuration has a naked singularity.

Because \mathcal{H} is a global entity, the legitimacy of using a linear mass distribution to model the behavior of the EH for a ring is not clear. As we argue below, the EH must be very close to the linear singularity when the line is sufficiently long, and hence its structure is, at least partially, dependent on the same singular behavior in the metric as the EH around the ring singularity. In addition, the spacetime near the singularity rapidly approaches flat space in both configurations. So outgoing null generators far enough away from the singularity to see the differences in the metric are also likely to be far enough

away to escape to infinity.

The study of the EH structure from a linear distribution is interesting in its own right, and if we can show that this distribution does not have a non-singular horizon in the distant past (which is supported by the work of [73]), this helps support the conjecture that any linear distribution, sufficiently extended in space, is surrounded by a singular horizon, or no horizon at all.

3. Numerical Techniques

We evolved these BH configuration using the LAZEV [78] implementation of the moving puncture approach [2, 3]. We obtain accurate horizon parameters by evolving this system in conjunction with a modified 1+log lapse and a modified Gamma-driver shift condition [2, 79], and an initial lapse $\alpha(t = 0) = 2/(1 + \psi_{BL}^4)$, we also used $\alpha(t = 0) = 1$ for the continuum ring. The lapse and shift are evolved with

$$(\partial_t - \beta^i \partial_i) \alpha = -2\alpha K, \quad (5)$$

$$\partial_t \beta^a = 3/4(\tilde{\Gamma}^a - \tilde{\Gamma}^a(0)). \quad (6)$$

When searching for EHs, we evolved these configuration using the unigrid PUGH driver [80]. After saving the metric at each timestep, we used the EHFINDER thorn [69] to locate the event horizons. In this case, we used the PUGH driver because the publicly available version of EHFINDER was not compatible with the CARPET AMR driver [81]. When evolving the continuum ring configuration, we used the CARPET driver because the resolutions required near the ring would have made a unigrid simulation prohibitively expensive. We used the AHFINDERDIRECT [82] thorn to locate apparent horizons.

In order to make the unigrid runs more efficient, we mimicked fixed-mesh-refinement using a multi-transition FishEye transformation [78, 79, 83]. In addition to this, we also exploited ‘octant symmetry’ in most of our simulations, allowing us to increase the resolution.

Solving the Einstein Equations for a BH ring of arbitrary radius numerically is not feasible due to resolution constraints. To understand why this is, we can consider the case of a discrete ring of some large radius. As we add more BHs to the ring, the mass of each BH is reduced. The resolution required to evolve a BH is inversely proportional to its mass, hence in the continuum limit, we would need an infinitesimal gridspacing. On the other hand, if a spheroidal common apparent horizon is present, then we only need

to resolve the region outside the AH. Thus, we can evolve ring configurations with small radii.

When searching for EHs using EHFinder [69] we first perform a standard forward in time evolution, outputting the full 4-d metric at every timestep, until the remnant BH is nearly spherical. We then perform a backwards in time evolution and track the null generators of the EH from the final AH backwards in time. As noted above, once two generators cross they leave the EH. Thus we need to remove these generators for all timesteps prior to their crossing. In practice, we do this by tracking the separation of each pair of generators, removing the pair if they get within a predetermined tolerance δ of each other. In practice we used $\delta \sim 10^{-4} - 10^{-5}$ (depending on the number of punctures). This tolerance is at least two or three orders of magnitude smaller than the spatial resolution used for evolving the system.

4. Results

4.1. Continuum Ring

For the continuum ring we evolved configurations with increasing ring radii using a set of fixed nested grids (FMR) with the Carpet mesh refinement driver.

We found that the resolution required to find the AH on the initial slice increases with the size of the ring (keeping the mass fixed). We were able to find AHs on the initial timeslice for rings with radii as large as $0.5M$. Based on axisymmetric simulations [75, 76], we know that AHs exist for rings of larger radii, but we were not able to find these initial AHs in our full 3d simulations due to a lack of spatial resolution. Even though we were unable to find an initial AHs numerically, we were still able to evolve ring configurations with radii as large as $1M$. On the other hand, an evolution of a ring with radius larger than $r \approx 1.2M$ was not possible even at high resolutions. Essentially, the logarithmic singularity in the metric disappears numerically due to the effects of finite differencing. That is, the evolution variable $W \sim 1/\log^2 R$, which is not differentiable. As is, this would not be a significant problem, but for large rings, the volume where W is close to zero is very small (see Fig. 3). Consequently W gets smoothed out in this region by finite-difference errors, and the central object quickly loses mass and disappears (and subsequent evolution show no evidence of collapse or an apparent horizon). For intermediate radii of $0.5 < r \leq 1.0M$, we were able to evolve the ring. In these cases, the ring collapsed and eventually a common AH was found.

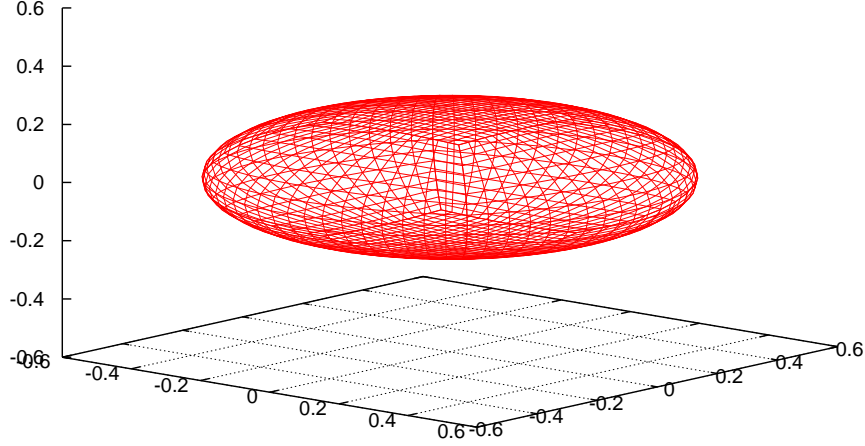


Figure 2. An early apparent horizons for a “continuum ring” singularity of radius 0.5 and unit mass. The AH is clearly an oblate spheroid with largest radius on the xy axis, corresponding to the plane of the ring singularity.

We used a 3d-Cartesian coordinate grid with outer boundaries at $100M$, with 3 ghost and 3 buffer zones, 8 levels of refinements. We found that the apparent horizons for the ring singularity are oblate spheroids with minor axes through the perpendicular direction to the plane of the ring, i.e. coincident with the axis of the ring (Fig. 2). We found that for ring radii larger than $0.5M$, the ring failed to collapse and essentially evaporated numerically. By changing the initial lapse to $\alpha(t = 0) = 1$ we were able to evolve rings with radii as large as $\sim 1.0M$. However, this changed the AH at intermediate times from oblate to prolate. This would seem to indicate that $\alpha(t = 0) = 1$ leads to a distorted z coordinate during intermediate times. In all cases, the AH relaxed to a sphere at late times. We note that the AH area always increased from its initial value (or the value found at the first time the AH was detected). We did not search for EH for the continuum ring because we were unable to evolve rings of sufficient radius to have interesting EHs.

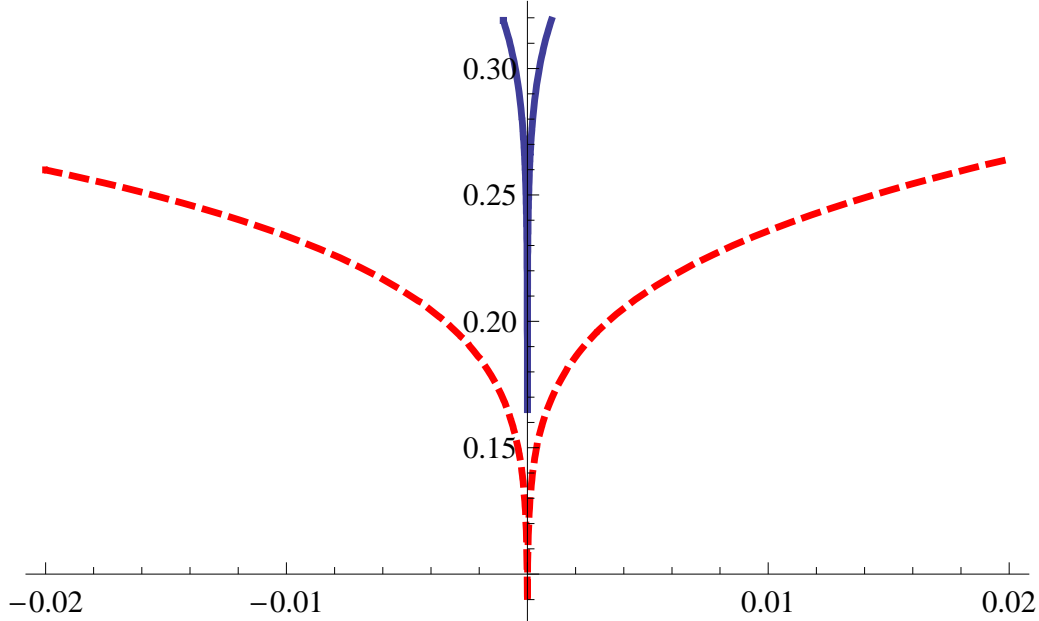


Figure 3. A plot of $W = 1/\psi^2$ versus $\tilde{\rho} = \rho - \rho_0$ on the xy plane for a ring of radius $1M$ (dashed) and $2M$ (solid). Note how much smaller the region $W < 0.3$ is for the larger ring radius. Based on the figure we estimate that an order 100 times the resolution is required to properly resolve the $r = 2M$ ring.

4.2. Discrete Ring

We evolved the discrete ring case in order to gain insight into the behavior of continuum rings with large radii (where numerical simulations are not feasible). The moving puncture approach has already been shown to work for large numbers of discrete punctures [84–86], and is therefore well suited for simulating the discrete case. The goal here was to see if, when we increase the number of BHs in the ring, while keeping the ring mass and radius fixed, a common horizon forms. In practice, we evolved configurations with $N = 2, 4, 6, 8, 10, 20$ BHs.

For the cases of $N = 10$ and 20 BHs, the overhead of using a unigrid setup was too large. We performed some preliminary experiments calculating AHs using Carpet and FMR. However, we were not able to search for EHs. For these cases, we simulated rings with radii as large as $2.5M$. As expected, initially there were N distinct AHs, which then merged into a common AH,

For $N = 2, 4, 6, 8$, in order to find the EHs we used a unigrid setup (a requirement

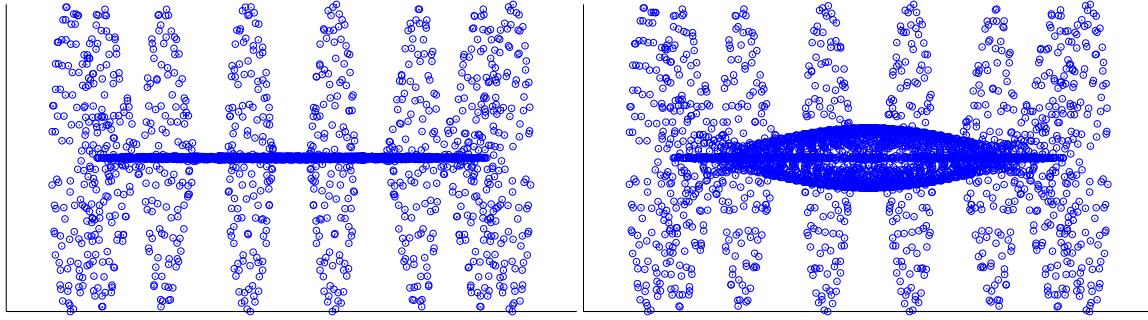


Figure 4. An edge-on view of the ‘pancaking’ of the central part of the EH for 8 BHs on a ring. The figure on the left shows the generators of the horizon at the timestep when the central generators just pass through the caustic and enter the horizons. The figure on the right shows the generators one timestep later. In the figure on the left, the central generators are just crossing (thus are not part of \mathcal{H} , while in the figure on the right an extended central object is visible. Note that the z axis is magnified by a factor of 10 compared to the x and y axes.

for the EHFinder thorn) with outer boundaries at a coordinate distance of $12.5M$, which corresponds to a physical distance of $45M$ due to the FishEye coordinates. Because the BH mass, and hence the required maximum gridspacing, scales as $1/N$, we used resolutions of $h = M/12$ and $h = M/16$ for $N = 2$, $h = M/24$ and $h = M/32$ for $N = 4$, and $h = M/48$ for $N = 6, 8$. In all the cases the Courant factor was set to 0.5. We varied the radius of the ring from $1.0M$ to $2.5M$.

In Fig. 4 we show the 8-BH discrete ring EH at the instant when the horizon transforms from 8 distinct objects to a single distorted horizon of topology S^2 , as well as the horizon at one timestep later when there is only a single EH. As noted above, the EH is actually found by a backward in time evolution. From this perspective, we note how the central part of the horizon ‘pancakes’ to zero width during a single timestep. Also note that the central part of the horizon is concave, indicating that the generators near $(x, y) = 0$ will not cross first. Thus a “hole” will not form and the EH (in this slicing) will not have a toroidal topology. In Figs. 6 and 5 we show xy projections and xz cuts of the same 8 BH configuration, while in Fig. 7 we show 3-d plots of the EHs (for $z \geq 0$). In Fig. 8 we show a sequence of $t = \text{const}$ slices of the EH, arranged vertically, to show the “octopus” like structure of this EH. Similar results for 4 and 6 BHs show that no central “hole” forms at any time.

Although we found no toroidal slice here, the caustic structure of the horizons

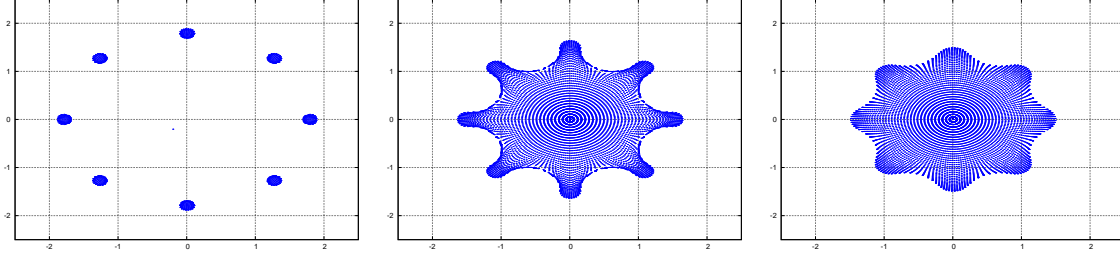


Figure 5. xy projections of the 8 BH ring configuration showing a time sequence with (left) 8 individual EHs, (center) a highly distorted common EH, (right) and a less distorted common EH.

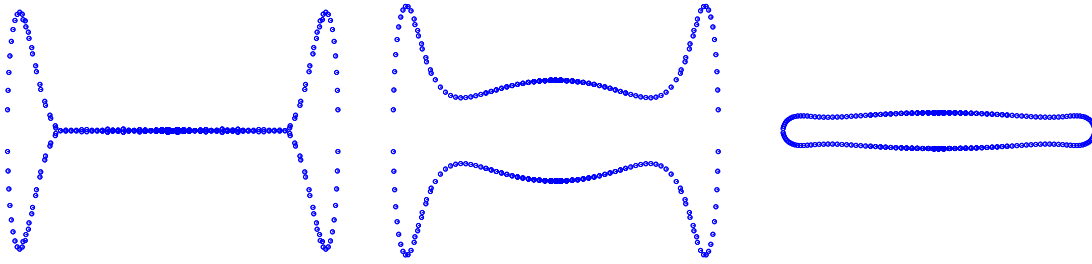


Figure 6. xz cuts of EH for the 8BH ring configuration at the instant in time when the common EH forms (left), two timesteps later (center, note the concave shape of the central region), and five timesteps after that (right). Note that the z axis in the two leftmost figures is magnified by a factor of 10 compared to the x axis, while the z scale is equal to the x scale in the last figure.

indicates that a toroidal slice is possible. That is, the caustic forms a 2-d spacelike *plane*, and a minor distortion of the slicing should produce a new slice that is slightly more advanced in a small volume outside the origin than it is at the origin itself. For example, one could try to modify the right-hand-side of Eq. (5) by adding a term of the form $-f(t) \exp[-(r/\sigma)^2]$, which should retard the slicing around the origin, leading to a toroidal slice (see Fig. 9).

4.3. Linear BH

As a test of conjecture that a black hole ring is not surrounded by a finite-sized toroidal horizon (for sufficiently large ring radii), we simulated the case where a differential line element of the ring can be approximated by a finite line segment. In other words, in order

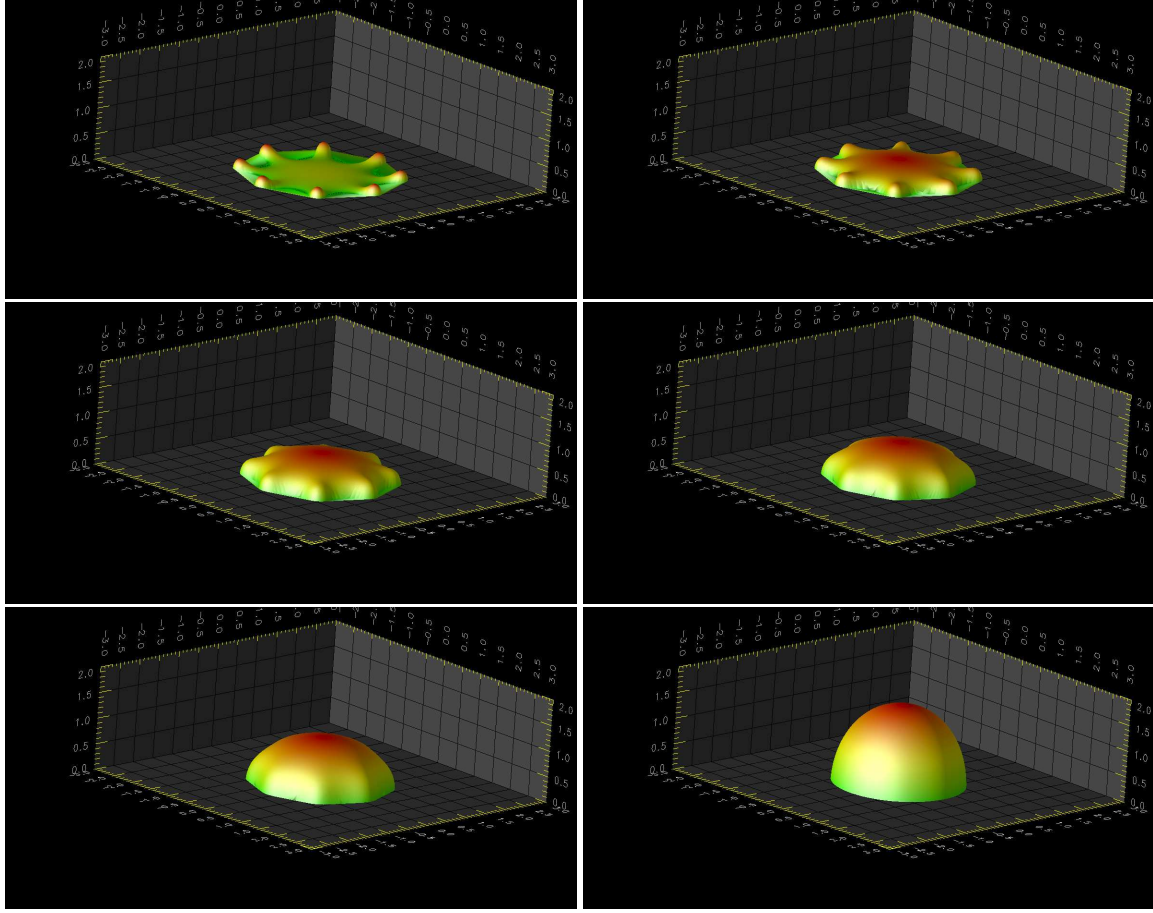


Figure 7. 3-d snapshots of the 8 BH ring configuration (only the top part of the horizon ($z \geq 0$) is shown). The sequence in time runs from left to right and top to bottom, beginning with the first common horizon and forward in time from then to when the horizon is nearly spherical. Note that the flat (green) sheet apparent between the horizon on the first and second slices is an artifact of the visualization and does not belong to the horizon. This provides another way to visualize the ‘pancaking’ process also visible in Figs. 4 and 6.

for there to be a common EH in the discrete ring case (with sufficiently large ring radius) a single EH must surround two neighboring punctures as the number of punctures becomes very large. In which case, a small section of the ring will look like a linear distribution of BHs. The question then is, if we have a finite length linear distribution of BHs of fixed total mass, will a common horizon form if the number of punctures in the line is increased arbitrarily, while keeping the total mass of the line fixed. In order to keep the linear mass

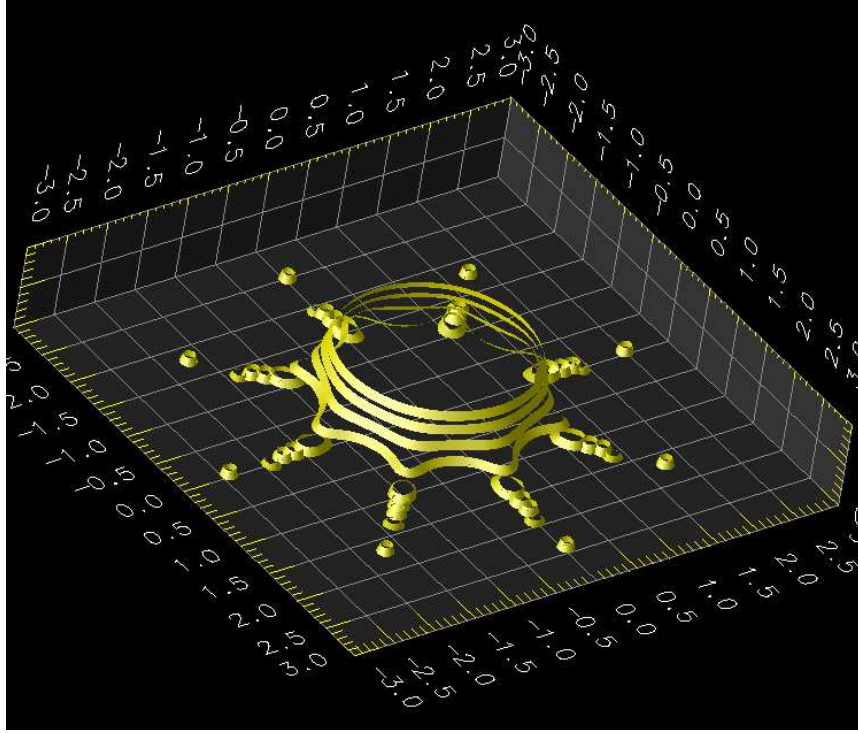


Figure 8. A sequence of $t = \text{const}$ slices of EH for the 8 BH ring configuration arranged vertically to show the “octopus” like structure of the EH

density constant as we change the number of BHs on the line (N), the length of the line element is given by Eq. (4).

There are two important objections to our modeling of the ring distribution with a linear distribution. First, because the metric on the initial slice is obtained by solving an elliptical equation, the notion that a linear mass distribution will mimic the relevant regions of the spacetime near a ring distribution requires some justification. Second, because the event horizon is a global structure, the global differences between the two spacetimes can cause the two event horizons to have very different property.

Our argument for using this linear distribution model goes as follows, as we move backwards in time and the ring gets larger, the event horizon must get progressively closer to the ring. This is due to the fact that the conformal factor ψ approaches 1 (and hence the metric rapidly approached Minkowski) progressively more rapidly as the ring radius is increased (see Fig. 3). Therefore \mathcal{H} gets progressively closer to the ring as the ring radius

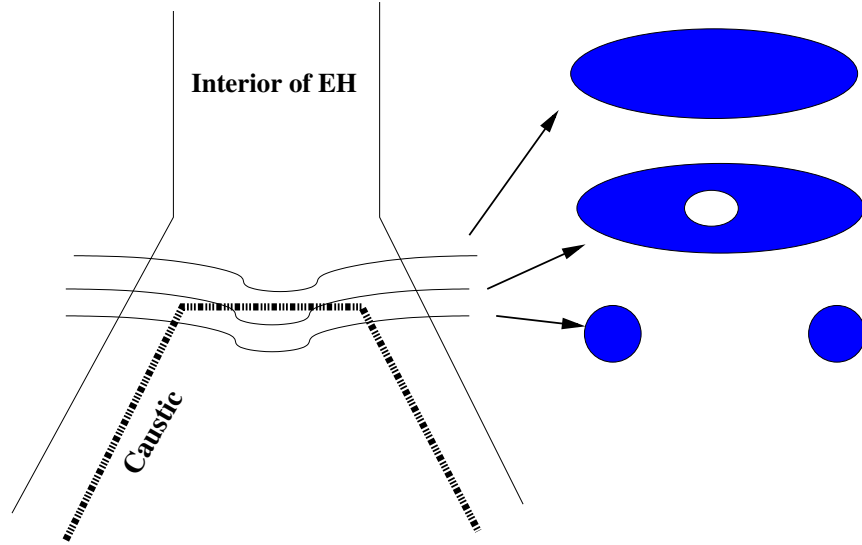


Figure 9. The caustic structure for the multiple black holes arranged on a ring. Only the tx plane is shown. From the figure, one can see that a toroidal horizon is possible if the slicing near the origin is retarded.

is increased. Indeed, because the region where ψ differs significantly from 1 shrinks very rapidly as the ring radius increases, the horizon radius must tend to zero faster than the reciprocal of the ring radius. Otherwise the outgoing null generators would enter a region where the space was nearly Minkowski and, due to the rapid falloff of ψ would therefore be able to escape to infinity. Consequently, for a large enough ring, the horizon will lie in a region where the metric is dominated by the singular $\log R$ term in ψ and will look like the metric in the vicinity of a linear mass distribution. As noted above, due to the global nature of the event horizon, it is not clear how precise the correspondence is between the horizon structure of the line and the ring. Consequently our results for the linear distribution should only be considered suggestive of the behavior of the horizon around the ring.

With the aim of numerically testing the conjecture that no finite sized EH exists for the distant past in the continuum ring case, we ran simulations with different values of N . First we determined the minimal distance between two black holes to generate two isolated (non-connected) event horizons in their initial configuration. We found that for a system of 2 black holes with total mass $M = 1.0$, the minimal separation between the BHs is $\approx 0.9M$. Given this, we then proceeded to evolve configurations for $N = 4$ with a line

length of $4.0M$ (which guarantees that no common EH exists initially). We then increased the number of BHs on the line and measured the coordinate separation of the two central holes as a function of N . For this analysis, we rescaled this inter-BH separation by the reciprocal of the individual BH masses. That is, the separation will decrease as N increases naturally because there are more BHs on the line, but we are interested in whether or not the EHs will merge as N increases. If the EHs merge then the separation l of the EHs will approach $2r$, where r is the EH radius. If on the other hand l/r tends to a constant larger than 2, as was the case here, then no common EH will form. Since the BH masses, and therefore coordinate radii, are proportional to $1/N$, we rescale the distances by a factor of N .

In Fig. 10, we plot the intersection of \mathcal{H}_t with the xy plane for the 10 BH line configuration for several different times. Interestingly, the two central BH merge first, followed by the two BHs neighboring the central ones, followed by the outermost ones. At one time there are three distinct EH formed by the two outermost EH on either side (2 objects) of the line and the 6 central objects (1 object).

In Figure 11 we show the EHs at $t \approx 0$ for the linear distribution with $N = 4, 6, 8$, and 10 BHs uniformly distributed over a line with length given by Eq. (4), i.e. lengths: 4.0, 4.444, 4.667, 4.8. For these evolution we used resolutions of $M/16$, $M/32$, $M/40$, and $M/50$ for $N = 4$, $N = 6$, $N = 8$, and $N = 10$, respectively. Due to an instability in the EH search, we could not find EHs at exactly $t = 0$ in all cases. In Figs. 12 and 13 we show only the two innermost EHs.

According to these figures, there is a clear trend towards reducing the effective size of the event horizons while keeping their separations, relative to the individual BH radius, fixed when increasing N (see for instance Fig. 13). This suggests that for finite N there will be N distinct BHs rather than a common EH. Thus for the limiting case $N \rightarrow \infty$, the event horizons would seem to have at most point like width, giving in the most optimistic scenario a null-width connected ring.

This setup was examined using an axisymmetric code with up to 1000 BHs arranged on a line in Ref. [73]. In that paper it was found that no common AH exists for lines longer than $1.5M$. Here we have extended this argument (somewhat) to no common event horizon for lines larger than $4M$ (we did not do a systematic study to determine the minimum line length for the existence of a common event horizon as a function of the number of BHs).

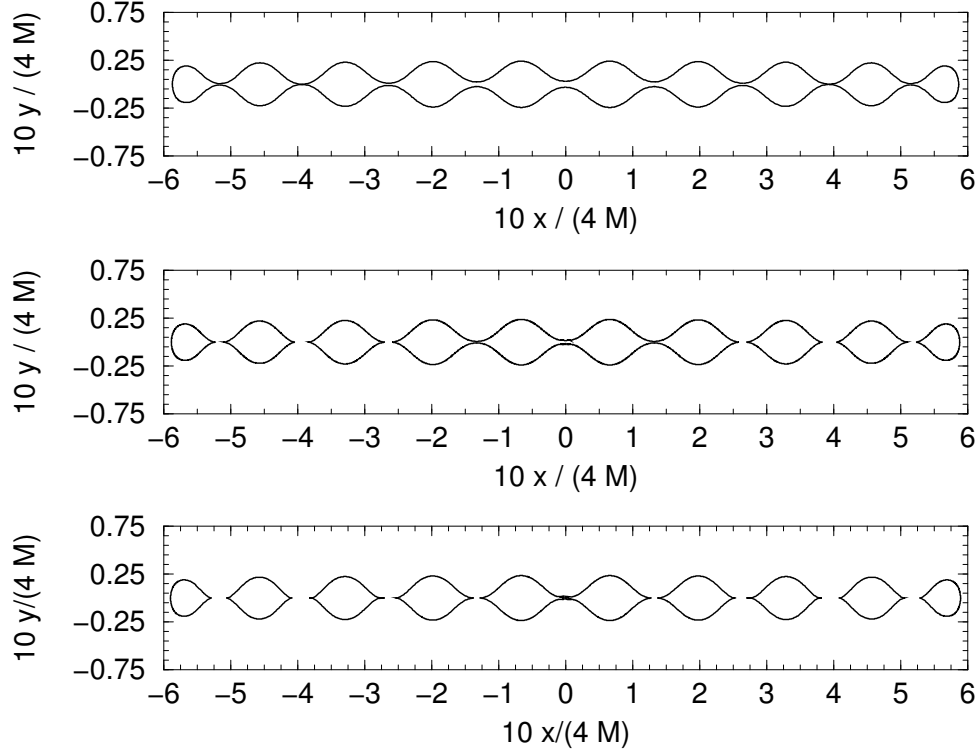


Figure 10. $t = \text{const}$ slices of the intersection of \mathcal{H} and the xy plane for the 10 black hole line configuration. The figure on top shows the first common EH, the figure in the center shows an earlier slice with 7 distinct objects, while the figure on the bottom shows the EH when there are 9 distinct objects. Note that the two central BHs merge first.

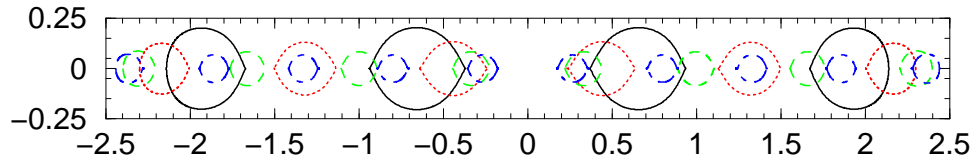


Figure 11. Sets of EHs near $t = 0$ for the linear distribution with $N = 4$ (solid), $N = 6$ (dotted), $N = 8$ (dashed), and $N = 10$ (dot-dashed) BHs. In this plot the coordinates have not been rescaled. Note that as N increases the two innermost horizons approach each other, but also simultaneously shrink in size.

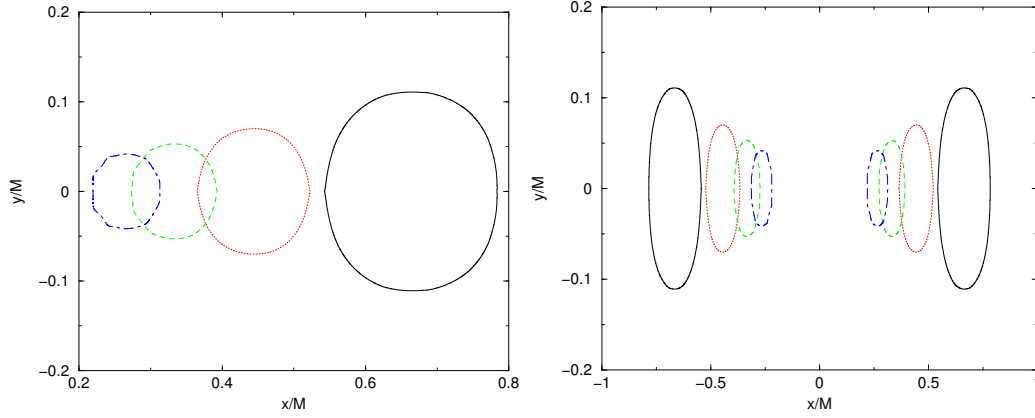


Figure 12. The two innermost EHs near $t = 0$ for the linear distribution with $N = 4$ (solid), $N = 6$ (dotted), $N = 8$ (dashed), and $N = 10$ (dot-dashed) BHs. In this plot the coordinates have not been rescaled. Note that as N increases the two innermost horizons approach each other, but also simultaneously shrink in size.

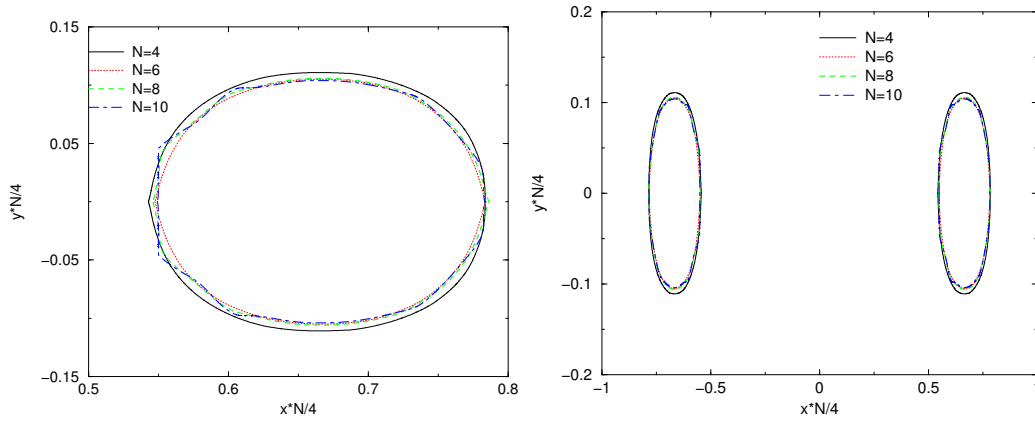


Figure 13. The two innermost EHs near $t = 0$ for the linear distribution with $N = 4$ (solid), $N = 6$ (dotted), $N = 8$ (dashed), and $N = 10$ (dot-dashed) BHs. Note that the distances have been scaled by $N/4$ and that the innermost horizons do not appear to approach each other as N increases.

5. Discussion

It is important to note that, unlike the case of discrete punctures, where the puncture singularities are only coordinate singularities, the singularities for these continuum linear distributions are physical singularities. We can show this by noting that the initial hypersurfaces are not geodesically complete. In the vicinity of a linear distribution, the conformal factor ψ will behave like $\psi \sim \log \rho$, where ρ is the coordinate distance to the line. Consequently, the physical distance of a point ρ away from the line is $\delta s \sim \rho \log^2 \rho$, which is finite. Next we note that the Kretschmann invariant $K = R_{\alpha\beta\gamma\delta}R^{\alpha\beta\gamma\delta}$ is singular and of the form $K \sim 1/[\rho^4(\log \rho)^{10}]$.

We can strengthen the argument for a non-simply connected EH in the continuum ring configuration (for large enough radius). We expect that the ring singularity will undergo gravitational collapse to a point. That is, the ring radius in quasi-isotropic coordinates will decrease with time. We therefore expect that the radius will get larger the farther back we move in time (one could also consider a family of initial data, where the mass of the ring is fixed to $1M$ but the radius is made arbitrarily large).

Suppose that there is an S^2 slice of \mathcal{H} surrounding the ring at all times. The surface area of the horizon will become arbitrarily large (we note that metric in the neighborhood of the ring is only logarithmically singular, and approaches Minkowski rapidly with the distance from the ring. This means that the spacetime will be very nearly Minkowski, including in the center of the ring) in the distant past (see Fig. 14). Thus if the ring is surrounded by an S^2 horizon in the distant past, the spacetime will be asymptotically predictable (i.e. posses at least a partial Cauchy surface) and should evolve to a Schwarzschild BH with surface area at least as big as the surface of the horizon when the ring is arbitrarily large (i.e. for the very distant past). However, this is not possible because the ring's mass is fixed, and hence its the horizons area is bounded. Consequently, the EH, if it exists, cannot be S^2 . We note that our tests with discrete ring configuration, and ring singularities with small radii, all indicate that the horizon area increases with time (as required). The increase in area is quite dramatic for the discrete ring. This is due to fact that the configuration does not radiate significantly, so the initial horizon masses are approximately equal to the total mass divided by the number of black holes. Hence the area of each horizon is proportional equal to $16\pi(M/N)^2$ and the total initial area is equal to $16\pi M^2/N$, or $1/N$ times the final horizon area. In the limit $N \rightarrow \infty$ this leads to an initial horizon with vanishing area.

We note that our results from the discrete ring configuration suggests that the EH, if

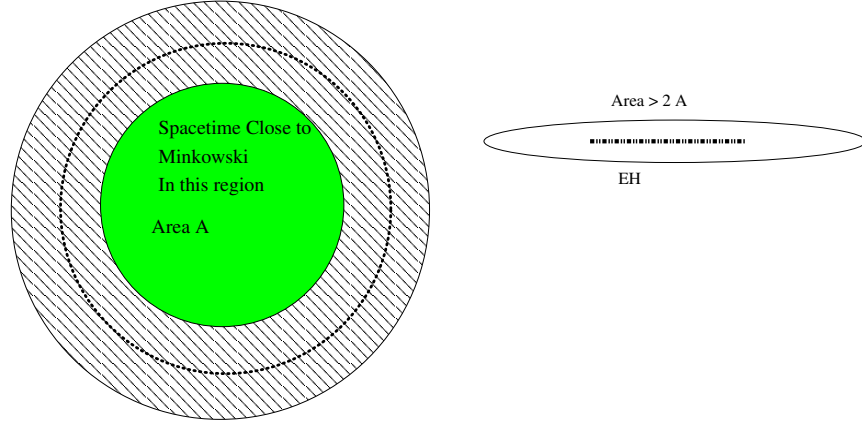


Figure 14. The conjectured S^2 horizon outside the ring singularity (dotted line) for a ring singularity with large radius. The shaded region is a region inside the ring but still far enough from the singularity that the metric is nearly flat. The surface area of this region is proportional to the square of the ring's radius, and hence get arbitrarily large. The horizon's area must be larger than twice this area. The plot on the left shows a cut on the xy plane, while the plot on the right shows a cut on the xz plane.

it exists, may have vanishing width. If this is so, then null geodesics originating arbitrarily close to the singularity (and hence in regions of arbitrarily large curvature) are visible to null infinity \mathcal{I}^+ , indicating the presence of a type of naked singularity, and the spacetime itself may not be asymptotically predictable (the presence of a naked singularity does not preclude that the spacetime is asymptotically predictable). While a horizon \mathcal{H}_t with a stable toroidal topology does not appear to exist for the ring singularity, the caustic structure of \mathcal{H} indicates that instantaneous toroidal slices are possible. Here the spacetime has no common EH at sufficiently early timeslices and only first appears at a timeslice Σ_h as an extended object with topology S^2 . However, because $\mathcal{H} \cap \Sigma_h$ is an extended object, Σ_h can be distorted to an alternate slice $\tilde{\Sigma}_h$ such that $\tilde{\Sigma}_h \cap \mathcal{H}$ is not simply connected (e.g. by distorting the timeslice such that the center of the ring is slightly earlier in time than the neighboring points). See Fig. 9.

Although we started by looking for configurations with EHs with toroidal slices, we actually have a more interesting case of a ring singularity with an EH in the future of some slice Σ_0 and a possible naked singularity in the past of Σ_0 . Although, in the slicing used here, the horizon appears to not have toroidal topology, we note that the slicing can be distorted to produce a toroidal horizon. This configuration appears to be a very interesting

topic for further analytical investigations.

Acknowledgments

We thank J.Friedman, Badri Krishnan and Peter Diener for helpful discussions. We thank the referees of this paper for their valuable advice and suggested revisions. We gratefully acknowledge NSF for financial support from grant PHY-0722315, PHY-0653303, PHY-0714388, PHY-0722703, DMS-0820923, PHY-0929114, and PHY-0969855; and NASA for financial support from grant NASA 07-ATFP07-0158 and HST-AR-11763. Computational resources were provided by Ranger cluster at TACC (Teragrid allocations TG-PHY080040N and TG-PHY060027N) and by NewHorizons at RIT.

References

- [1] Pretorius F 2005 *Phys. Rev. Lett.* **95** 121101 (*Preprint* gr-qc/0507014)
- [2] Campanelli M, Lousto C O, Marronetti P and Zlochower Y 2006 *Phys. Rev. Lett.* **96** 111101 (*Preprint* gr-qc/0511048)
- [3] Baker J G, Centrella J, Choi D I, Koppitz M and van Meter J 2006 *Phys. Rev. Lett.* **96** 111102 (*Preprint* gr-qc/0511103)
- [4] Lindblom L, Scheel M A, Kidder L E, Owen R and Rinne O 2006 *Class. Quant. Grav.* **23** S447–S462 (*Preprint* gr-qc/0512093)
- [5] Gundlach C and Martin-Garcia J M 2006 *Phys. Rev.* **D74** 024016 (*Preprint* gr-qc/0604035)
- [6] van Meter J R, Baker J G, Koppitz M and Choi D I 2006 *Phys. Rev.* **D73** 124011 (*Preprint* gr-qc/0605030)
- [7] Campanelli M, Lousto C O and Zlochower Y 2006 *Phys. Rev. D* **74** 041501(R) (*Preprint* gr-qc/0604012)
- [8] Campanelli M, Lousto C O and Zlochower Y 2006 *Phys. Rev. D* **74** 084023 (*Preprint* astro-ph/0608275)
- [9] Campanelli M, Lousto C O, Zlochower Y, Krishnan B and Merritt D 2007 *Phys. Rev.* **D75** 064030 (*Preprint* gr-qc/0612076)
- [10] Rezzolla L *et al.* 2008 *Astrophys. J.* **674** L29–L32 (*Preprint* arXiv:0710.3345[gr-qc])
- [11] Sperhake U *et al.* 2008 *Phys. Rev.* **D78** 064069 (*Preprint* 0710.3823)
- [12] Dain S, Lousto C O and Zlochower Y 2008 *Phys. Rev. D* **78** 024039 (*Preprint* 0803.0351)
- [13] Dreyer O, Krishnan B, Shoemaker D and Schnetter E 2003 *Phys. Rev.* **D67** 024018 (*Preprint* gr-qc/0206008)
- [14] Schnetter E, Krishnan B and Beyer F 2006 *Phys. Rev.* **D74** 024028 (*Preprint* gr-qc/0604015)
- [15] Cook G B and Whiting B F 2007 *Phys. Rev.* **D76** 041501 (*Preprint* arXiv:0706.0199[gr-qc])
- [16] Krishnan B, Lousto C O and Zlochower Y 2007 *Phys. Rev.* **D76** 081501 (*Preprint* 0707.0876)
- [17] Campanelli M, Lousto C O and Zlochower Y 2009 *Phys. Rev. D* **79** 084012 (*Preprint* 0811.3006)
- [18] Owen R 2010 *Phys. Rev.* **D81** 124042 (*Preprint* 1004.3768)

- [19] Herrmann F, Hinder I, Shoemaker D M, Laguna P and Matzner R A 2007 *Phys. Rev.* **D76** 084032 (Preprint 0706.2541)
- [20] Marronetti P *et al.* 2007 *Class. Quant. Grav.* **24** S43–S58 (Preprint gr-qc/0701123)
- [21] Marronetti P, Tichy W, Brugmann B, Gonzalez J and Sperhake U 2008 *Phys. Rev.* **D77** 064010 (Preprint 0709.2160)
- [22] Berti E *et al.* 2007 *Phys. Rev.* **D76** 064034 (Preprint gr-qc/0703053)
- [23] Herrmann F, Shoemaker D and Laguna P 2006 *AIP Conf.* **873** 89–93 (Preprint gr-qc/0601026)
- [24] Baker J G *et al.* 2006 *Astrophys. J.* **653** L93–L96 (Preprint astro-ph/0603204)
- [25] González J A, Sperhake U, Brugmann B, Hannam M and Husa S 2007 *Phys. Rev. Lett.* **98** 091101 (Preprint gr-qc/0610154)
- [26] Herrmann F, Hinder I, Shoemaker D, Laguna P and Matzner R A 2007 *Astrophys. J.* **661** 430–436 (Preprint gr-qc/0701143)
- [27] Campanelli M, Lousto C O, Zlochower Y and Merritt D 2007 *Astrophys. J.* **659** L5–L8 (Preprint gr-qc/0701164)
- [28] Campanelli M, Lousto C O, Zlochower Y and Merritt D 2007 *Phys. Rev. Lett.* **98** 231102 (Preprint gr-qc/0702133)
- [29] Lousto C O and Zlochower Y 2009 *Phys. Rev. D* **79** 064018 (Preprint 0805.0159)
- [30] Pollney D *et al.* 2007 *Phys. Rev.* **D76** 124002 (Preprint 0707.2559)
- [31] González J A, Hannam M D, Sperhake U, Brugmann B and Husa S 2007 *Phys. Rev. Lett.* **98** 231101 (Preprint gr-qc/0702052)
- [32] Brugmann B, Gonzalez J A, Hannam M, Husa S and Sperhake U 2008 *Phys. Rev.* **D77** 124047 (Preprint 0707.0135)
- [33] Choi D I *et al.* 2007 *Phys. Rev.* **D76** 104026 (Preprint gr-qc/0702016)
- [34] Baker J G *et al.* 2007 *Astrophys. J.* **668** 1140–1144 (Preprint astro-ph/0702390)
- [35] Schnittman J D *et al.* 2008 *Phys. Rev.* **D77** 044031 (Preprint 0707.0301)
- [36] Baker J G *et al.* 2008 *Astrophys. J.* **682** L29 (Preprint 0802.0416)
- [37] Healy J *et al.* 2009 *Phys. Rev. Lett.* **102** 041101 (Preprint 0807.3292)
- [38] Herrmann F, Hinder I, Shoemaker D and Laguna P 2007 *Class. Quant. Grav.* **24** S33–S42
- [39] Tichy W and Marronetti P 2007 *Phys. Rev.* **D76** 061502 (Preprint gr-qc/0703075)
- [40] Koppitz M *et al.* 2007 *Phys. Rev. Lett.* **99** 041102 (Preprint gr-qc/0701163)
- [41] Miller S H and Matzner R A 2009 *Gen. Rel. Grav.* **41** 525–539 (Preprint 0807.3028)
- [42] Boyle L, Kesden M and Nissanke S 2008 *Phys. Rev. Lett.* **100** 151101 (Preprint 0709.0299)
- [43] Boyle L and Kesden M 2008 *Phys. Rev.* **D78** 024017 (Preprint 0712.2819)
- [44] Buonanno A, Kidder L E and Lehner L 2008 *Phys. Rev.* **D77** 026004 (Preprint arXiv:0709.3839[astro-ph])
- [45] Tichy W and Marronetti P 2008 *Phys. Rev.* **D78** 081501 (Preprint 0807.2985)
- [46] Kesden M 2008 *Phys. Rev.* **D78** 084030 (Preprint 0807.3043)
- [47] Barausse E and Rezzolla L 2009 *Astrophys. J. Lett.* **704** L40–L44 (Preprint 0904.2577)
- [48] Rezzolla L 2009 *Class. Quant. Grav.* **26** 094023 (Preprint 0812.2325)
- [49] Lousto C O, Campanelli M, Zlochower Y and Nakano H 2010 *Class. Quant. Grav.* **27** 114006 (Preprint 0904.3541)
- [50] Buonanno A, Cook G B and Pretorius F 2007 *Phys. Rev.* **D75** 124018 (Preprint gr-qc/0610122)

- [51] Baker J G, van Meter J R, McWilliams S T, Centrella J and Kelly B J 2007 *Phys. Rev. Lett.* **99** 181101 (Preprint gr-qc/0612024)
- [52] Pan Y *et al.* 2008 *Phys. Rev.* **D77** 024014 (Preprint arXiv:0704.1964[gr-qc])
- [53] Buonanno A *et al.* 2007 *Phys. Rev.* **D76** 104049 (Preprint arXiv:0706.3732[gr-qc])
- [54] Hannam M, Husa S, Sperhake U, Bruegmann B and Gonzalez J A 2008 *Phys. Rev.* **D77** 044020 (Preprint 0706.1305)
- [55] Hannam M, Husa S, Bruegmann B and Gopakumar A 2008 *Phys. Rev.* **D78** 104007 (Preprint 0712.3787)
- [56] Gopakumar A, Hannam M, Husa S and Bruegmann B 2008 *Phys. Rev.* **D78** 064026 (Preprint 0712.3737)
- [57] Hinder I, Herrmann F, Laguna P and Shoemaker D 2010 *Phys. Rev.* **D82** 024033 (Preprint 0806.1037)
- [58] Gonzalez J A, Sperhake U and Bruegmann B 2009 *Phys. Rev.* **D79** 124006 (Preprint 0811.3952)
- [59] Lousto C O, Nakano H, Zlochower Y and Campanelli M 2010 *Phys. Rev. Lett.* **104** 211101 (Preprint 1001.2316)
- [60] Friedman J L, Schleich K and Witt D M 1993 *Phys. Rev. Lett.* **71** 1486–1489 (Preprint gr-qc/9305017)
- [61] Hawking S W 1972 *Commun. Math. Phys.* **25** 152–166
- [62] Hawking S W and Ellis G F R 1973 *The Large Scale Structure of Spacetime* (Cambridge, England: Cambridge University Press)
- [63] Galloway G J and Schoen R 2006 *Commun. Math. Phys.* **266** 571–576 (Preprint gr-qc/0509107)
- [64] Galloway G J 2006 (Preprint gr-qc/0608118)
- [65] Racz I 2008 *Class. Quant. Grav.* **25** 162001 (Preprint 0806.4373)
- [66] Hughes S A *et al.* 1994 *Phys. Rev.* **D49** 4004–4015
- [67] Shapiro S L, Teukolsky S A and Winicour J 1995 *Phys. Rev.* **D52** 6982–6987
- [68] Husa S and Winicour J 1999 *Phys. Rev.* **D60** 084019 (Preprint gr-qc/9905039)
- [69] Diener P 2003 *Class. Quant. Grav.* **20** 4901–4918 (Preprint gr-qc/0305039)
- [70] Cohen M I, Pfeiffer H P and Scheel M A 2009 *Class. Quant. Grav.* **26** 035005 (Preprint 0809.2628)
- [71] Shapiro S L and Teukolsky S A 1991 *Phys. Rev. Lett.* **66** 994–997
- [72] Shapiro S L and Teukolsky S A 1992 *Phys. Rev. D* **45** 2006–2012
- [73] Abrahams A M, Heiderich K R, Shapiro S L and Teukolsky S A 1992 *Phys. Rev.* **D46** 2452–2463
- [74] Lehner L and Pretorius F 2010 *Phys. Rev. Lett.* **105** 101102 (Preprint 1006.5960)
- [75] Jaramillo G and Lousto C O 2010 (Preprint 1008.2001)
- [76] Wojtkiewicz J 1990 *Phys. Rev. D* **41** 1867–1874
- [77] Brill D and Lindquist R 1963 *Phys. Rev.* **131** 471–476
- [78] Zlochower Y, Baker J G, Campanelli M and Lousto C O 2005 *Phys. Rev. D* **72** 024021 (Preprint gr-qc/0505055)
- [79] Alcubierre M, Brügmann B, Diener P, Koppitz M, Pollney D, Seidel E and Takahashi R 2003 *Phys. Rev. D* **67** 084023 (Preprint gr-qc/0206072)
- [80] Cactus Computational Toolkit home page: <http://www.cactuscode.org>
- [81] Schnetter E, Hawley S H and Hawke I 2004 *Class. Quantum Grav.* **21** 1465–1488 (Preprint gr-qc/0310042)

- [82] Thornburg J 2004 *Class. Quantum Grav.* **21** 743–766 (*Preprint* gr-qc/0306056)
- [83] Baker J, Campanelli M and Lousto C O 2002 *Phys. Rev. D* **65** 044001 (*Preprint* gr-qc/0104063)
- [84] Campanelli M, Lousto C O and Zlochower Y 2008 *Phys. Rev. D* **77** 101501(R) (*Preprint* 0710.0879)
- [85] Lousto C O and Zlochower Y 2008 *Phys. Rev.* **D77** 024034 (*Preprint* 0711.1165)
- [86] Galaviz P, Brugmann B and Cao Z 2010 *Phys. Rev.* **D82** 024005 (*Preprint* 1004.1353)